All the complexes have an additional unusual property. They can be heated in vacuo to produce a purple high-spin Fe(II) product, which when dissolved in aromatic hydrocarbons in air reforms the $(FeL)_2O$ dimer. The weight loss is consistent in each case with (1). This is the first case of a reversal of such an Fe–O–Fe linkage, e.g., the very similar oxo-bridged dimers formed with such ligands as the tetradentate salen and its cbp analogue, are simply destroyed by heating. The purple products of reaction 1 rapidly gain weight when exposed to air and then are invariably

$$(FeL)_2O\cdot n(\text{solvent}) \underset{\text{xylene}}{\overset{190\ ^\circ\text{C, vac}}{\rightleftharpoons}} 2FeL(+{}^1/{}_2O_2) + n(\text{solvent}) \tag{1}$$

analyzed as $FeL\cdot O_2$, and in no case does either the infrared or the hydrogen analysis support the presence of water. The nature of these complexes, presumable Fe(II) from the magnetism and spectra, has not yet been established. They are inaccessible to X-ray crystallography at this stage: on dissolving in hydrocarbon solvents, they revert to the red$(FeL)_2O$ complexes. The data are given for the L = cbpN case in Tables I and II.

The magnetically coupled $(FeL)_2O$, formed when the high-spin iron(II) $[FeL]\cdot nH_2O$ (e.g., $[Fe(cbpN)]\cdot 2H_2O$, Tables I and II) is recrystalled from benzene or a substituted benzene solvent, is stable in air at room temperature in the solid state, but the binucleation is reversed in freshly distilled dimethylacetamide: a purple solution is obtained and the spectrum reverts to that of $Fe^{II}L$ parent. This is presumable because the highly substituted ligand exerts sufficient steric crowding to make the Fe–O–Fe linkage somewhat unstable, but not sufficient to prevent it forming at all, as with the highly substituted porphyrins and other ligands used in synthetic oxygen carriers.[22–24]

While $(FeL)_2O$ is an acceptable model for the hemerythrin magnetic properties, it is not a good hemerythrin model otherwise. In fact none such yet exist. It does carry a half-molecule of oxygen with partial reversibility, but it does not carry dioxygen. However, it is a good model for the PIG iron site (in its oxidized form) to the extent that the latter is understood: it is a nonheme, nonporphyrin system, containing O-donor atoms in addition to the μ-oxo bridge and the magnetic coupling. An important step in a further understanding of the enzyme is in mimicking some of its salient properties in model complexes such as the ones described. The model is supported by observation of similar magnetic properties[25] in the purple phosphatase from beef spleen.[3] It must therefore be considered that not only this enzyme but also the purple acid phosphatases from plant sources[26] may have similar Fe_2 centers.

The magnetic, ESR, and crystallographic measurements were made as described elsewhere.[1,2,27]

Registry No. Fe(cbpN), 84752-95-4; $[Fe(cbpN)O_2]$, 84775-37-1; $[(Fe(cbpN))_2O]$, 84752-94-3; acid phosphatase, 9001-77-8.

Supplementary Material Available: Tables of interatomic distances and angles, fractional coordinates, and thermal parameters for $[(Fe(cbpN))_2O]\cdot 3xyl$ (11 pages). Ordering information is given on any current masthead page.

---

[22] Leal, O.; Anderson, D. L.; Bowman, R. G.; Basolo, F.; Burwell, R. L.., Jr. *J. Am. Chem. Soc.* **1975**, *97*, 5125.

[23] Little, R. G.; Ibers, J. A.; Baldwin, J. E. *J. Am. Chem. Soc.* **1975**, *97*, 7049.

[24] Collman, J. P.; Gagne, R. R.; Reed, C. A.; Robinson, W. T.; Rodley, G. A. *Proc. Natl. Acad. Sci.* U.S.A. **1974**, *71*, 1326.

[25] Averill, B. A., personal communcation.

[26] Nochumson, S.; O'Rangers, J. J.; Dimitrov, N. V. *Fed, Proc., Fed. Am. Soc. Exp. Biol.* **1974** *33*, 1378. Sugiura, Y.; Kawabe, H.; Tanaka, H. *J. Am. Chem. Soc.* **1980**, *102*, 6581. Fujimoto, S.; Nakagawa, T.; Ishimitsu, S.; Ohara, A. *Chem. Pharm. Bull.* **1977**, *25*, 1459. Fujimoto, S.; Nakagawa, T.; Ohara, A. *Ibid.* **1977**, *25*, 3283. Igaue, I.; Watanabe, H.; Takahashi, K.; Takekoshi, M.; Morata, A. *Agric. Biol. Chem.* **1976**, *40*, 823.

[27] Freyberg, D. P.; Mockler, G. M.; Sinn, E. *J. Chem. Soc.*, Dalton *Trans.* **1976**, 447.

Paramagnetic Organometallic Molecules. 13.[1] Electron-Transfer-Catalyzed Reactions of Polynuclear Metal Carbonyls: Reactions of $R_2C_2Co_2(CO)_6$

Malini Arewgoda, Brian H. Robinson,* and Jim Simpson*

Contribution from the Department of Chemistry, University of Otago, Dunedin, New Zealand.

Received August 12, 1982

Abstract: Polynuclear metal carbonyls are shown to be suitable substrates for rapid electron-transfer-catalyzed (ETC) reactions that offer a new convenient method for the synthesis of many carbonyl derivatives. The factors that influence the applicability and yields of these reactions are discussed and examples with a variety of nucleophiles and substrates given. The distinction between electron-induced nucleophilic substitution (EINS) and ETC reactions is emphasized. ETC reactions of $R'RC_2Co_2(CO)_6$ with MeCN and other Lewis bases using both electrolytic and chemical reductants are described in detail, in particular those where R′ = R = CF_3. The yields of the new products $(CF_3)_2C_2Co_2(CO)_5L$ [L = MeCN, $(MeO)_3P$, $(PhO)_3P$, Ph_3P, $(C_6H_{11})_3P$], $(CF_3)_2C_2Co_2(CO)_4L_2$ [L = $(RO)_3P$, Ph_3P], and $(CF_3)_2C_2Co_2(CO)_3L_3$ [L = $(RO)_3P$] are virtually quantitative, with reaction times no longer than 5 min. In most cases reaction is over in 1 min at 293 K. Yields from ETC reactions with other $R'RC_2Co_2(CO)_6$ compounds are variable but can be correlated with the lifetime of the radical anions. Spectroscopic data characterized the phosphite or phosphine ligand as having an axial conformation in $R_2C_2Co_2(CO)_5L$ complexes, but the X-ray structure of $(CF_3)_2C_2Co_2(CO)_5(MeCN)$ shows that the MeCN is equatorial. Steric factors are believed to account for this. However, the MeCN ligand is very labile in solution, and the electrochemistry of the MeCN adduct is characterized by abnormal limiting currents at 293 K that are absent at lower temperatures. The compound $(CF_3)_2C_2Co_2(CO)_5(MeCN)$ crystallizes in the space group $Pna2_1$; $a = 15.794$ (5) Å, $b = 9.803$ (3) Å, $c = 10.936$ (4) Å, $Z = 4$, $V = 1693.4$ Å^3.

Electron-transfer catalysis is a general class of reaction in which electron-transfer steps are utilized to accelerate transformations which are slow under normal thermal conditions and/or to alter product distribution.[2] A unimolecular mechanism $S_{RN}1$ for

0002-7863/83/1505-1893$01.50/0 © 1983 American Chemical Society

Scheme I

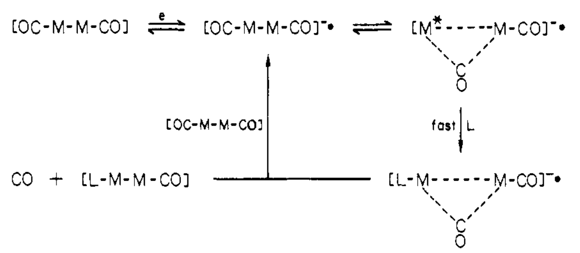

nucleophilic substitution has been recognized in a number of systems with organic substrates.[3]

$$[RX]^{-}\cdot \rightarrow R\cdot + X^{-} \qquad (1)$$

$$R\cdot + Y^{-} \rightarrow [RY]^{-}\cdot \qquad (2)$$

$$[RY]^{-}\cdot + RX \rightarrow RY + [RX]^{-}\cdot \qquad (3)$$

Providing RX is an easily reduced substrate and forms a relatively long-lived radical anion and the electron transfer (3) is rapid, then a chain process is developed and the electron-induced nucleophilic substitution may be called[2] electron-transfer chain catalyzed (ETC). Polynuclear metal carbonyl substrates can be shown to fulfill the requirements of the ETC process.[4-7]

Radical anions of polynuclear metal carbonyls have been studied in some detail,[8-10] and as we will show, the additional electron enables these species to act as substrates for ETC reactions. Because the HOMO is both ligand and metal in character,[11] and the LUMO metal in character,[9,11,12] the HOMO–LUMO separation (measured by $E°$) is reduced in energy by the removal of charge on the metal atoms by the π-acid ligands, and in many cases reduction potentials are quite low.[13,14] Many carbonyl radical anions are persistent and in some cases can be isolated and their structures determined.[15] As a general rule the lifetime of the radical anion decreases as the electronegativity of the groups on the metal cluster core (whether bound to the metal or as capping function on the cluster) decreases. A corollary is that the lifetime of capped metal cluster radical anions is significantly longer than that of noncapped;[16] bimolecular fragmentation pathways are less accessible in the former (vide infra). Thus, one criterion for ETC reactions, namely reversible radical anion formation, is satisfied by polynuclear metal carbonyls.

Dissociation of the electron-rich radical anion into radicals and anions, which forms the basis of the $S_{RN}1$ mechanism for organic substrates, is not a feasible mechanistic pathway for polynuclear metal carbonyls, with the possible exception of hydrides. Similarly, bimolecular nucleophilic attack on the coordinatively saturated electron-rich cluster radical anions is an unlikely alternative. The impetus for the direct electron-induced nucleophilic substitution of the radical anions of polynuclear metal carbonyls is expected to come from their particular electronic structure. These radical anions are characterized by the odd electron occupying an antibonding orbital centered on the metal core, and we have suggested that an activated intermediate is accessible because of the consequential weakening of the metal–metal bond (Scheme I).[1,5]

Ultimately, bond stretching in the activated complex would produce a coordinatively unsaturated 17-electron metal atom (M*) which will be activated to nucleophilic attack.[17] The precise ordering of events and relative rates for CO dissociation and nucleophilic addition is difficult to judge on the data currently available[18] (this point is discussed in more detail later for $(CF_3)_2C_2Co_2(CO)_6$ as substrate). Nevertheless, the very fact that the rate of nucleophilic attack on radical anions is increased by a factor of $>10^6$ compared to the neutral substrate and that the spectral data show that the M–CO bond is thermodynamically stronger in the radical anions does indicate that metal–metal bond "cleavage" in the activated complex would provide a pathway for an $S_{RN}1$ mechanism.

The final condition for an ETC process as distinct from an electron-induced substitution—that the chain-propagating step be spontaneous—is satisfied when CO is replaced by most nucleophiles because the increased charge density on the metal atom causes a negative shift in the one-electron reduction potential.[13,14] Yields from ETC reactions will be dependent on the lifetime of the radical anion compared with the rate of electron transfer. The most important modes of radical anion decomposition are disproportionation and fragmentation, and both of these chain-terminating steps are minimized where there is a capping function across the metal core or at low temperatures. Electron transfer has been shown to be intrinsically fast with polynuclear metal carbonyl substrates.[16] However, this outer-sphere transfer is believed to take place via a CO group and one can envisage a range of electron-transfer rates influenced by the stereochemical nuances of the cluster and ligands. Furthermore, ion pairing and cation–anion association certainly mediate electron-transfer rates[19] and electrode processes for metal carbonyl clusters[16] and would therefore have an important role in ETC reactions.

The ETC process can be seen to offer an exciting opportunity to develop a new synthetic tool for metal carbonyl chemistry, but it should be emphasized that an ETC mechanism, as outlined

---

(1) Part 12. Arewgoda, M.; Robinson, B. H.; Simpson, J.; Rieger, P. H.; Visco, S. J. *J. Am. Chem. Soc.* **1982**, *104*, 5633–5640.

(2) Alder, R. W. *J. Chem. Soc., Chem. Commun.* **1980**, 1184–1186. Chanon, M.; Tobe, M. L. *Angew. Chem., Int. Ed. Engl.* **1982**, *21*, 1–86.

(3) (a) Bunnett, J. F. *Acc. Chem. Res.* **1978**, *11*, 413–420. (b) Beletskaya, I. P.; Drozd, V. N. *Russ. Chem. Rev. (Engl. Transl.)* **1979**, *48*, 431–448. (c) Saveant, J.-M. *Acc. Chem. Res.* **1980**, *13*, 323–329. Amatore, C.; Pinson, J.; Saveant, J.-M.; Thiebault, A. *J. Am. Chem. Soc.* **1982**, *104*, 817–826.

(4) The possibility of electron-induced nucleophilic substitution with tricobalt carbon clusters has been considered by Rieger and co-workers[5] and the concept of ETC reactions briefly considered by us,[1] Darchen,[6] Kochi,[7a] and Wrighton[7b] as applied to organometallic molecules.

(5) (a) Bezems, G. J.; Rieger, P. H.; Visco, S. J. *J. Chem. Soc., Chem. Commun.* **1981**, 265–266. (b) Bruce, M. I.; Kehoe, D. C.; Matisons, J. G.; Nicholson, B. K.; Rieger, P. H.; Williams, M. L. *Ibid.* **1982**, 442–444.

(6) Darchen, A.; Mahe, C.; Patin, H. *J. Chem. Soc., Chem. Commun.* **1982**, 243–244.

(7) (a) Hershberger, J. W.; Kochi, J. K. *J. Chem. Soc., Chem. Commun.* **1982**, 212–214. (b) Summers, D. P.; Luong, J. C.; Wrighton, M. S. *J. Am. Chem. Soc.* **1981**, *103*, 5238.

(8) (a) Matheson, T. W.; Peake, B. M.; Robinson, B. H.; Simpson, J. *J. Chem. Soc., Chem. Commun.* **1973**, 894–895. (b) Peake, B. M.; Robinson, B. H.; Simpson, J.; Watson, D. J. *Ibid.* **1974**, 945–946. (c) Peake, B. M.; Robinson, B. H.; Simpson, J.; Watson, D. J. *Inorg. Chem.* **1977**, *16*, 405–410. (d) Dickson, R. S.; Peake, B. M.; Rieger, P. H.; Robinson, B. H.; Simpson, J. *J. Organomet. Chem.* **1979**, *172*, C63–C65. (e) Dawson, P. A.; Peake, B. M.; Rieger, P. H.; Robinson, B. H.; Simpson, J. *Inorg. Chem.* **1980**, *19*, 465–472.

(9) Peake, B. M.; Rieger, P. H.; Robinson, B. H.; Simpson, J. *Inorg. Chem.* **1981**, *20*, 2540–2543.

(10) (a) Illenda, C. S.; Shore, N. E.; Bergman, R. G. *J. Am. Chem. Soc.* **1976**, *98*, 256–258. (b) Krusic, P. J.; Filappo, J. S.; Hutchinson, B.; Hance, R. L.; Daniels, L. M. *Ibid.* **1981**, *103*, 2129–2131.

(11) (a) Thorn, D. L.; Hoffmann, R. *Inorg. Chem.* **1978**, *17*, 126–140. (b) Schilling, B. E. R.; Hoffmann, R. *J. Am. Chem. Soc.* **1978**, *100*, 6274. (c) Hall, R. B. *Inorg. Chem.* **1981**, 4419–4425.

(12) (a) Peake, B. M.; Rieger, P. H.; Robinson, B. H.; Simpson, J. *J. Am. Chem. Soc.* **1980**, *102*, 156–163. (b) Peake, B. M.; Rieger, P. H.; Robinson, B. H.; Simpson, J. *Inorg. Chem.* **1979**, *18*, 1000–1005.

(13) Bond, A. M.; Dawson, P. A.; Peake, B. M.; Rieger, P. H.; Robinson, B. H.; Simpson, J. *Inorg. Chem.* **1979**, *18*, 1413–1417.

(14) (a) Peake, B. M.; Robinson, B. H.; Simpson, J.; Watson, D. J. *Inorg. Chem.* **1977**, *16*, 410–415. (b) Bond, A. M.; Dawson, P. A.; Robinson, B. H.; Simpson, J. *Ibid.* **1977**, *16*, 2199–2203.

(15) For example, crystalline samples of $Na(crypt\text{-}222)^{+}[PhCCo_3(CO)_9]^{-}\cdot$ are stable in air for several hours apart from surface oxidation to $PhCCo_3(CO)_9$, and a crystal of this radical anion will initiate ETC reactions.[16]

(16) Lindsay, P. N. T.; Robinson, B. H.; Simpson, J.; Vahrenkamp, H. *Inorg. Chem.*, submitted for publication. Lindsy, P. N. T. Ph.D. Thesis, University of Otago, 1982.

(17) Brown, T. L. *Ann. N.Y. Acad. Sci.* **1980**, *333*, 80–89.

(18) Darchen and co-workers[6] have questioned whether metal–metal cleavage is an integral part of ETC reactions with polynuclear carbonyls. For reasons which are elaborated in the Discussion of this paper, we prefer this mechanism to one involving dissociative loss of CO.

(19) Kirk, C.; Peake, B. M.; Robinson, B. H.; Simpson, J. *Aust. J. Chem.*, in press.

Table I. New $(CF_3)_2C_2Co_2(CO)_6$ Derivatives

	found			calcd				
L	C	H	P(N)	C	H	P(N)	ν(CO),^{a} cm^{-1}	^{1}H
				$(CF_3)_2C_2Co_2(CO)_5L$				
CH_3CN	28.72	0.93	(2.93)	28.66	0.66	(3.03)	2108 s, 2072 vs, 2052 vs, 2028 vs	2.30 s^b
$(MeO)_3P$	27.79	2.29	5.51	26.49	1.67	5.69	2098 s, 2052 vs, 2042 b, 2016 s	3.70 d
$(PhO)_3P$	43.93	2.18	4.32	44.38	2.05	4.25	2096 s, 2052 vs, 2041 vs, 2018 s	7.13 m
Ph_3P	47.22	2.64		47.51	2.20	4.55	2094 s, 2052 s, 2038 b, 2001 s	7.43 m
$(C_6H_{11})_3P$	46.34	4.89		46.29	4.71	4.43	2101 s, 2048 vs, 2032 b, 2001 s	1.45 m
				$(CF_3)_2C_2Co_2(CO)_4L_2$				
$(MeO)_3P$	26.24	3.05	9.42	26.26	2.83	9.67	2056 w, 2043 s, 2017 vs, 1997 vs	3.63 m
$(PhO)_3P$	52.12	3.14	6.18	52.17	2.96	6.13	2055 m, 2039 vs, 2014 vs, 1985 vs	7.10 m
Ph_3P	57.93	3.88		57.64	3.30	6.77	2050 s, 2025 vs, 2001 vs, 1977 w	7.37 m
				$(CF_3)_2C_2Co_2(CO)_3L_3$				
$(MeO)_3P$	26.17	4.30	13.95	26.10	3.69	12.62	2036 s, 1986 b	3.60 m^c
$(PhO)_3P$	56.43	3.71	7.20	56.57	3.48	7.19	2035 s, 1980 b	7.10 m
				$(CF_3)_2C_2Co_2(CO)_2L_4$				
$(MeO)_3P$	26.96	4.59	14.53	25.97	4.36	14.88	1980 s, 1956 b	3.58 s, b
$(PhO)_3P$	59.45	3.72	7.51	59.39	3.81	7.87	1975 s, 1953 b	7.11 m

^{a} In hexane. ^{b} ^{19}F NMR, see text. ^{c} ^{19}F 30.99 m, 31.50 m.

Table II. Yields from ETC Reactions with $RC_2R'Co_2(CO)_6$ to Form $RC_2R'Co_2(CO)_{6-n}L_n$

	yield			
L	BPK	E^a	T^b	current efficiency^c
	R = R' = CF_3; n = 1			
CH_3CN	100	70	38	960
$P(OMe)_3$	100	100	80	3100
PPh_3	90	85	67	2100
$P(C_6H_{11})_3$	90	83	48	1520
	n = 2			
$P(OMe)_3$		94^d	70	864
PPh_3		60^d	28	512
	n = 3			
$P(OMe)_3$		64^d	30	460
	R = H, R' = CF_3; n = 1			
$P(OMe)_3$	84	79	75	1700
PPh_3	67	65	53	870
$P(C_6H_{11})_3$	41	49	51	520
	R = H, R' = ^{t}Bu; n = 1			
$P(OMe)_3$	61	74	69	456
PPh_3	42	17	54	159
$P(C_6H_{11})_3$	3	2	13	33
	R = H, R' = Ph; n = 1			
$P(OMe)_3$	27	36	72	220
PPh_3	8	15	50^e	61
$P(C_6H_{11})_3$	<1	4	19	31
	R = Ph, R' = Ph; n = 1			
$P(OMe)_3$	<5	20	85^e	
PPh_3	<1	8	84^e	
$P(C_6H_{11})_3$	<1	<5	15^e	

^{a} Electrolysis using the trigger potential of the appropriate $RC_2R'Co_2(CO)_6^{-}\cdot$. Radical anion with a slight excess of the required amount of ligand. ^{b} Thermal preparation in boiling hexane under nitrogen for 3 h. ^{c} Coulometry, moles of product per faraday of charge passed. ^{d} Small amounts of lower-substituted derivatives are also produced; yields quoted are based on an optimum mole ratio of ligand; for n = 2 this was 1:2.5 substrate:ligand and for n = 3, 1:3.5. ^{e} Yields from ref 21.

above, is a specific case of the more general class of electron-induced nucleophilic substitution (EINS) which may or may not be catalytic. With EINS it is not necessary for substitution that the polynuclear metal carbonyl satisfy the strict requirements of an ETC process. Provided the radical anion is thermodynamically accessible, then synthetically advantageous reactions can be achieved, even if the kinetic stability of the radical anion is not attractive. For a genuine ETC mechanism to be the dominant pathway, the rate of nucleophilic attack on the activated radical anion of the metal carbonyl species must be exceptionally fast relative to the chain-terminating steps; in this case current efficiency (if electrochemically triggered) is high, the number of faradays consumed per mole of substrate approaches zero, and the substrate/chemical reductant mole ratio is extremely high. At the other extreme, noncatalytic electron-induced nucleophilic substitution is characterized by lower current efficiencies, faraday/mol ratios approaching unity, and product yields which will depend on the concentration of the reductant. Most metal carbonyl–nucleophile systems will most likely fall somewhere between these extremes, and it is essential that electrochemical studies accompany synthetic work.

Detailed electrochemical studies described earlier[1] provide the background to the electron-induced reactions with $RC_2R'Co_2(CO)_6$ complexes as substrates given in this paper. This particular system is one where the ETC process can be studied as a function of the lifetime of the radical anion and nucleophilic reactivity, and both chemical reductants and an electrode can be used as chain initiators. In addition, examples of electron-induced nucleophilic substitution reactions of polynuclear metal carbonyls are described, some of which are ETC processes.

Experimental Section

All reactions were carried out under nitrogen or argon unless stated otherwise. The complexes $RC_2R'Co_2(CO)_6$ were prepared by published procedures;[20] $P(OPh)_3$ (Strem), $P(OMe)_3$ (Strem), PPh_3 (BDH), and $P(C_6H_{11})_3$ (Strem) were used as received. Phosphine and phosphite derivatives of $Ph_2C_2Co_2(CO)_6$ were prepared by the methods described by Cullen et al.[21] Acetonitrile was stored over CaH_2 for several days with intermittent shaking; the decanted solvent was fractionally distilled from P_2O_5 and N_2 onto dry 3-Å molecular sieves. Solvent CH_2Cl_2 was washed 3 times with sodium hydroxide and 3 times with distilled water, dried over $CaCl_2$, and then distilled from CaH_2 and stored over molecular sieves. Other solvents were purified and dried by standard methods. Sodium naphthalenide was prepared by mixing a 1:1 molar ratio of sodium and naphthalene in deoxygenated tetrahydrofuran. A solution of benzophenone ketyl (BPK) was prepared by refluxing benzophenone in deoxygenated tetrahydrofuran with a slight molar excess of sodium; for most reactions, the solution was simply syringed from a still used to purify tetrahydrofuran.

Conventional DC polarograms and cyclic voltammograms were recorded on Princeton Applied Research equipment described previously.[14a] The potentiostat was a home-built model and, with the three-electrode system employed, the potential stability was ±0.01 V in a current range 0–100 mA. All potentials are with respect to a solid Ag/AgCl electrode. ^{1}H and ^{13}C NMR data were acquired on a 60-MHz JEOL C-60 HL or Perkin-Elmer spectrometer with an internal Me_4Si standard. ^{19}F NMR data were acquired on a 90-MHz JEOL spectrometer at the University of Waikato, Hamilton.

---

(20) Dickson, R. S.; Fraser, P. J. *Adv. Organomet. Chem.* **1974**, *12*, 323–341.

(21) Chia, L. S.; Cullen, W. R.; Franklin, M.; Manning, A. R. *Inorg. Chem.* **1975**, *14*, 2521–2526.

Analytical and spectroscopic data for $(CF_3)_2C_2Co_2(CO)_{6-n}L_n$ derivatives are given in Table I and yields and current efficiencies of ETC reactions in Table II.

Electrochemical Preparation of $(CF_3)_2C_2Co_2(CO)_5(CH_3CN)$. The electrochemical cell used for the syntheses described in this paper was a typical 150-cm^3 three-electrode cell with a Hg-pool cathode (25 cm^3); the auxillary electrode, a tightly coiled Pt wire, and the reference electrode were separated from the catholyte by methylcellulose gels containing electrolyte. The acetonitrile solution of supporting electrolyte (75 cm^3, 0.1 mol dm^{-3} Et_4NClO_4) was added to the cell, degassed, and preelectrolyzed at −0.8 V until the current decreased to a constant value. At this point the potential was reduced to −0.55 V and 0.5 g of $(CF_3)_2C_2Co_2(CO)_6$ was added to the solution (which was efficiently stirred by the gas flow). There was an immediate color change and the solution became a deep red as the current decreased. After 5 min TLC analysis showed that a trace of $(CF_3)_2C_2Co_2(CO)_6$ remained, but prolonged electrolysis caused decomposition rather than increased yields. The solvent was removed under reduced pressure, the residue extracted several times with ether, and the insoluble supporting electrolyte then removed by filtration. The filtrate was concentrated and chromatographed on a silica gel column. Elution with hexane removed the unreacted $(CF_3)_2C_2Co_2(CO)_6$ and the product was eluted with hexane–ether (4:1). Deep red crystals of (μ-1,2-bis(trifluoromethyl)ethyne)[dicarbonyl(acetonitrile)cobalt]tricarbonylcobalt(*Co–Co*), **1**, crystallized from the elutant, yield 0.36 g (70%). Mass spectra: The parent molecular ion was not observed but two major fragmentation series $(CF_3)_2C_2Co_2(CO)_n{}^+$ and $(CF_3)_2C_2Co_2(CO)_n(CH_3CN)^+$ (n = 0–4) were identified; secondary fragmentation occurred by the loss of fluorine atoms from dinuclear ions—fragmentation to mononuclear cobalt ions was negligible. The compound is stable in air and soluble in organic solvents. If the preparation is carried out under CO, yields are reduced to approximately 20%.

Preparation of $(CF_3)_2C_2Co_2(CO)_5(CH_3CN)$ Using Chemical Reductants. The complex $(CF_3)_2C_2Co_2(CO)_6$ (0.10 g) was dissolved in 20 cm^3 of CH_3CN and the solution flushed with argon for 2 min. Approximately 0.1 cm^3 of a deep blue tetrahydrofuran solution of benzophenone ketyl was introduced to the solution via an air-tight syringe. The concentration of the benzophenone ketyl was not critical as long as it has the characteristic deep blue color, neither was the amount added as it is essentially acting as a catalyst; as noted earlier, a convenient source of ketyl is a still for the purification of THF. On addition of the ketyl the solution became the deep red color of $(CF_3)_2C_2Co_2(CO)_5(CH_3CN)$, and TLC analysis showed that complete reaction has occurred after 1 min. The solvent was stripped in vacuo and the residue recrystallized from hexane to give (μ-1,2-bis(trifluoromethyl)ethyne][dicarbonyl(acetonitrile)cobalt]tricarbonylcobalt(*Co–Co*); yield 0.10 g (100%).

A similar procedure can be used with sodium naphthalenide as reductant.

Thermal Preparation of $(CF_3)_2C_2Co_2(CO)_5(CH_3CN)$. A solution of $(CF_3)_2C_2Co_2(CO)_6$ (0.1 g) in CH_3CN was refluxed for 3 h (TLC analysis showed that this maximized the yield), the solvent stripped in vacuo, and the residue purified by preparative thin-layer chromatography as described above. The yield of $(CF_3)_2C_2Co_2(CO)_5(CH_3CN)$ was 0.04 g (38%).

Crystal Structure of $(CF_3)_2C_2Co_2(CO)_5(CH_3CN)$. Purple-black needle-shaped crystals of $(CF_3)_2C_2Co_2(CO)_5(CH_3CN)$ were obtained by vacuum sublimation at room temperature. The dimensions of the needle used for data collection were 0.97 × 0.54 × 0.37 mm. Precession photography (Cu Kα) showed orthorhombic symmetry and the space group was confirmed as $Pna2_1$ by the success of the analysis. Crystal data: $(CF_3)_2C_2Co_2(CO)_5(CH_3CN)$, molar mass 401.0 g mol^{-1}; $Pna2_1$; a = 15.794 (5) Å, b = 9.803 (3) Å, c = 10.936 (4) Å; v = 1693.4 Å^3 Z = 4; d_c = 1.81 g cm^{-3}; μ(Mo Kα) = 21.25 cm^{-1}.

Data were collected with Zr-filtered Mo Kα radiation on a Hilger and Watts four-circle computer-controlled diffractometer in the θ–2θ scan mode. The intensities were corrected for Lorentz and polarization effects but no absorption corrections were applied. Of the 1174 reflections collected, 629 had values of $F_o{}^2$ that were greater than twice their estimated standard deviations and these were used in the final refinement of structural parameters. Structure solution and refinement: The structure was solved by direct methods with the program MULTAN.[22] The chosen E map revealed the location of the two cobalt atoms. A series of least-squares refinement and difference Fourier syntheses using the program SHELX[23] revealed the coordinates of the remaining non-hydrogen atoms. The two cobalt atoms were assigned anisotropic thermal parameters, a weighting scheme based on counting statistics was introduced and the refinement converged with R_1 = 0.0868 and R_2 = 0.0879.

Table III. Bond Lengths (Å) for $(CF_3)_2C_2Co_2(CO)_5(MeCN)^a$

Co1–Co2	2.465 (6)	C5–O5	1.129 (30)
Co1–C3	1.791 (38)	C6–O6	1.142 (27)
Co1–C4	1.780 (40)	C7–O7	1.021 (51)
Co1–N	1.908 (52)	C8–C9	1.561 (40)
Co1–C9	1.985 (40)	C8–F1	1.428 (82)
Co1–C10	1.906 (41)	C8–F2	1.266 (37)
Co2–C5	1.759 (26)	C8–F3	1.186 (55)
Co2–C6	1.768 (27)	C9–C10	1.347 (32)
Co2–C7	1.846 (46)	C10–C11	1.466 (38)
Co2–C9	1.899 (39)	C11–F4	1.396 (77)
Co2–C10	1.942 (42)	C11–F5	1.336 (58)
N–C1	1.194 (71)	C11–F6	1.313 (32)
C1–C2	1.545 (76)		
C3–O3	1.133 (36)		
C4–O4	1.143 (40)		

[a] Standard deviations in the least significant digit appear in parentheses in this and subsequent tables.

Table IV. Selected Angles (deg) for $(CF_3)_2C_2Co_2(CO)_5(MeCN)$

N–Co1–Co2	94.3 (20)	C2–C1–N	167.0 (68)
N–Co1–C3	98.0 (35)	O3–C3–Co1	168.7 (80)
N–Co1–C4	103.5 (36)	O4–C4–Co1	163.2 (101)
C3–Co1–Co2	155.0 (34)	O5–C5–Co2	164.1 (33)
C4–Co1–Co2	99.3 (36)	O6–C6–Co2	173.1 (36)
C4–Co1–C3	98.9 (47)	O7–C7–Co2	174.4 (45)
C9–Co1–Co2	49.1 (13)	F1–C8–C9	98.5 (44)
C9–Co1–C3	109.6 (35)	F2–C8–C9	109.0 (29)
C9–Co1–C4	103.7 (36)	F2–C8–F1	107.5 (51)
C9–Co1–N	137.2 (24)	F3–C8–C9	116.2 (41)
C10–Co1–Co2	50.8 (15)	F3–C8–F1	104.0 (37)
C10–Co1–C3	105.1 (36)	F3–C8–F2	119.0 (58)
C10–Co1–C4	142.0 (37)	Co2–C9–Co1	78.8 (9)
C10–Co1–N	101.8 (20)	C8–C9–Co1	125.0 (40)
C10–Co1–C9	40.4 (11)	C8–C9–Co2	147.0 (38)
C5–Co2–Co1	147.0 (14)	C10–C9–Co1	66.6 (23)
C6–Co2–Co1	98.7 (14)	C10–C9–Co2	71.2 (23)
C6–Co2–C5	101.9 (18)	C10–C9–C8	136.1 (30)
C7–Co2–Co1	100.9 (14)	Co2–C10–Co1	79.7 (9)
C7–Co2–C5	98.8 (17)	C9–C10–Co1	72.9 (23)
C7–Co2–C6	104.0 (18)	C9–C10–Co2	67.8 (23)
C9–Co2–Co1	52.2 (14)	C11–C10–Co1	133.9 (49)
C9–Co2–C5	97.7 (19)	C11–C10–Co2	138.5 (46)
C9–Co2–C6	103.5 (15)	C11–C10–C9	136.1 (24)
C9–Co2–C7	144.0 (18)	F4–C11–C10	110.4 (55)
C10–Co2–Co1	49.5 (14)	F5–C11–C10	113.3 (41)
C10–Co2–C5	99.9 (19)	F5–C11–F4	106.6 (29)
C10–Co2–C6	140.7 (18)	F6–C11–C10	113.5 (26)
C10–Co2–C7	104.4 (16)	F6–C11–F4	99.1 (43)
C10–Co2–C9	41.0 (10)	F6–C11–F5	112.8 (51)
C1–N–Co1	173.3 (52)		

High-temperature factors for the carbonyl and trifluoromethyl groups indicated the possibility of crystallographic disorder in the molecule. This was confirmed by careful inspection of a difference Fourier map which revealed areas of high electron density close to the oxygen and fluorine atoms. However, because of the limitations of the available data set, the disorder problem was not investigated further.

No abnormal discrepancies were found between observed and calculated structure factors for those reflections not used in the refinement, and the weighting scheme appeared reasonable. Final bond lengths are given in Table III and selected bond angles in Table IV.

Electrocatalytic Preparation of Phosphine and Phosphite Derivatives, $(CF_3)_2C_2Co_2(CO)_{6-n}L_n$ (n = 1–3). A typical procedure for the electrochemical preparations is as follows. Reduction of $(CF_3)_2C_2Co_2(CO)_6$ in the presence of excess $P(OMe)_3$ at −0.45 V was carried out as for the preparation of $(CF_3)_2C_2Co_2(CO)_5(CH_3CN)$ except that the current was only passed for approximately 1 min. TLC analysis showed that no reactant was left, and the solvent was stripped from the resultant deep red solution. A concentrated solution of the residue in CH_2Cl_2 was applied to 20 × 20 cm × 1.25 mm silica gel plates which were developed in hexane–ether (10:1) to three bands: 1, red-orange (R_f 0.31), 2, dark red (R_f 0.16), and 3, dark red (R_f 0.11). Band one was removed and eluted with hexane and the solvent evaporated in vacuo. The residue recrystallized from hexane to give small orange crystals of (μ-1,2-bis(trifluoromethyl)ethyne)[dicarbonyl(trimethyl phosphite)cobalt]tricarbonylcobalt(*Co–Co*), $(CF_3)_2C_2Co_2(CO)_5(MeO)_3P$, mp 65 °C.

---

(22) Main, P.; Woolfson, M. M.; Germain, G., MULTAN-74 suit of programs.

(23) Sheldrick, G. M., SHELX program for crystal structure determination, Cambridge, 1975.

Band two was similarly treated to give red-orange crystals of (μ-1,2-bis(trifluoromethyl)ethyne)bis(dicarbonyl(trimethyl phosphite)cobalt)-(*Co–Co*), $(CF_3)_2C_2Co_2(CO)_4[(OMe)_3P]_2$, when recrystallized at 0 °C; it exists as a red oil at room temperature. Band three was eluted with ether, the solvent stripped, and the residue recrystallized from hexane–CH_2Cl_2 to give dark red rhombs of (μ-1,2-bis(trifluoromethyl)-ethyne)[bis((trimethyl phosphite)carbonyl)cobalt]dicarbonyl(trimethyl phosphite)cobalt(*Co–Co*), $(CF_3)_2C_2Co_2(CO)_3[(MeO)_3P]_3$, mp 77 °C.

Other phosphine and phosphite derivatives were prepared by the same procedure and the products separated by preparative thin-layer chromatography (Table I). The product distribution is largely determined by the complex:ligand molar ratio and yields can be optimized by monitoring the reaction by TLC. If the current is passed from several minutes, there is an increase in the yield of the $n > 1$ derivatives but there is increased decomposition; the same trend is observed if the trigger potential is made more negative. In general, the total yield of products amounts to more than 80% based on $(CF_3)_2C_2Co_2(CO)_6$. Even with very high PPh_3:$(CF_3)_2C_2Co_2(CO)_6$ ratios, there was no indication, either in the infrared spectra or TLC, of a derivative with $n > 2$; similarly, there was no evidence for the formation of $(CF_3)_2C_2Co_2(CO)_2L_4$ (L = $(RO)_3P$) derivatives.

Chemical ETC Preparations of $(CF_3)_2C_2Co_2(CO)_{6-n}L_n$ Derivatives. A small volume (0.1 cm^3) of a deep blue THF solution of BPK was syringed into a THF solution of $(CF_3)_2C_2Co_2(CO)_6$ (0.2 g) and $(MeO)_3P$ (0.1 g) under argon. There was an immediate deepening of the red color, and a TLC analysis showed that the $(CF_3)_2C_2Co_2(CO)_6$ had been replaced by one product. The solution was immediately evaporated to dryness, and the residue separated on preparative TLC plates as described for the electrocatalytic preparation above. Yield of $(CF_3)_2C_2Co_2(CO)_5(MeO)_3P$, 0.24 g (100%).

When the relative concentration of $(MeO)_3P$ was increased, small yields of $(CF_3)_2C_2Co_2(CO)_4[(MeO)_3P]_2$ (from 10 to 40%) and a trace of $(CF_3)_2C_2Co_2(CO)_3[(MeO)_3P]_3$ were obtained with a compensatory decrease in the $n = 1$ derivative. Increasing the amount of BPK at the beginning of the reaction did not increase the yield of $n > 1$ derivatives. However, if the reaction solution is treated with a further aliquot of BPK after, say 2 min, there is an increase in the yield of $n > 1$ but this increase is rather variable. There is no doubt that the controlled potential catalytic route is more selective for the preparation of $n = 2$ and 3 derivatives.

Other phosphine and phosphite compounds ($n = 1$) were similarly prepared, but note that $n = 2$ phosphine derivatives were rarely isolated from BPK reactions. Yields of phosphite compounds are always ~100%, but slightly lower yields are found with phosphines (~80%).

Preparation of $(CF_3)_2C_2Co_2(CO)_5L$ (L = PR_3, $P(OR)_3$ from $(CF_3)_2C_2Co_2(CO)_5(CH_3CN)$). A solution of $(CF_3)_2C_2Co_2(CO)_5(CH_3CN)$ (0.1 g) and $(MeO)_3P$ (0.04 g) in hexane was stirred at room temperature for 10 min. The solution was concentrated and applied to a preparative silica gel plate; development in hexane–ether (10:1) gave only one orange band from which $(CF_3)_2C_2Co_2(CO)_5(MeO)_3P$ was obtained as orange crystals, yield 0.11 g (92%).

High yields (>90%) of other $(CF_3)_2C_2Co_2(CO)_5L$ derivatives were obtained by using the same procedure.

Thermal Preparation of $(CF_3)_2C_2Co_2(CO)_{6-n}L_n$. The thermal reactions of $(CF_3)_2C_2Co_2(CO)_6$ with phosphines or phosphites were carried out in boiling solvents by standard procedures.[21] After the solvent was stripped in vacuo, the orange-red residues were chromatographed on a Fluorosil column with diethyl ether–hexane mixtures as elutants, with the following results (yields are for the most highly substituted derivative under the particular conditions):

n	$(CF_3)_2C_2Co_2$-$(CO)_6$: $(OMe)_3P$ ratio	solvent	time, h	eluent, ether–hexane	yield, %
1	1:1.5	benzene	3	1:1	80
2	1:2.5	benzene	2	1:4	70
3	1:3.5	toluene	2	1:10	30
4	1:4.5	toluene	3	3:7	20

The procedure was similar with other ligands. The yields were considerably lower with PPh_3 than those with phosphite ligands and the $n = 3$ and $n = 4$ derivatives were not detected.

ETC Reactions of $Ph_2C_2Co_2(CO)_6$ and Other $R_2C_2Co_2(CO)_6$ Complexes. (a) $Ph_2C_2Co_2(CO)_6$ (0.1 g) in acetonitrile was electrolyzed at −0.82 V, as described for the preparation of $(CF_3)_2C_2Co_2(CO)_5(MeCN)$. TLC and infrared analysis during the electrolysis gave no indication that a MeCN adduct was being formed, and after 5 min, TLC analysis showed that the $Ph_2C_2Co_2(CO)_6$ had completely disappeared; the only carbonyl species left in solution was $Co(CO)_4^-$. At this point the solvent was stripped in vacuo and the residue extracted with hexane from which 15 mg of Ph_2C_2 was recovered (identified by mass spectrum and ^{1}H NMR spect); for complete decomposition of $Ph_2C_2Co_2(CO)_6$, the theoretical yield of Ph_2C_2 is 38 mg but no other organic product was identified. The residue, insoluble in hexane (and CH_2Cl_2), was inorganic and contained cobalt metal as well as Co(II) salts. If the electrolysis was carried out with a cylindrical Pt electrode as working electrode, rather than a Hg pool, cobalt metal was deposited on the electrode.

Similar results were obtained under a CO atmosphere and if the ETC reaction was carried out with a chemical reductant such as BPK.

(b) A small aliquot of BPK was added to a stirred solution of $Ph_2C_2Co_2(CO)_6$ (0.1 g) and $(MeO)_3P$ (excess) in THF (25 cm^3). The solution darkened immediately, and TLC analysis after 1 min indicated that a small amount of $Ph_2C_2Co_2(CO)_6$ remained unreacted; a hexane-soluble product had been formed but there was extensive decomposition. The solvent was removed in vacuo and the residue extracted with ether, and the extracts were chromatographed on preparative TLC plates, eluent ether–hexane. The product $Ph_2C_2Co_2(CO)_5[(MeO)_3P]$ was obtained as small red crystals, yield <10% (identified by analysis, infrared spectrum, and mp 84 °C). This is a much lower yield than obtained from thermal methods, but the yield can be increased to approximately 20% if electrolytic rather than chemical reduction is used.

Other phosphites gave similar yields with $Ph_2C_2Co_2(CO)_6$, but no derivatives are produced with monodentate phosphines such as Ph_3P or $(C_6H_{11})_3P$.

(c) The reactions described in (a) and (b) were also carried out with other substrates $R'RC_2Co_2(CO)_6$ (R′ = Ph, *t*-Bu, CF_3, R = H) with the results given in Table I. As a general rule the yields were higher than those with $Ph_2C_2Co_2(CO)_6$ and accompanied by less decomposition to $Co(CO)_4^-$, cobalt metal, and parent acetylene.

Results and Discussion

Electrochemistry of $RC_2R'Co_2(CO)_6$ in CH_3CN. A convenient solvent for ETC reactions is acetonitrile as it has a wide potential range, is easily purified and is unreactive toward chemical reducing agents, such as benzophenone ketyl. Since preparations in this donor solvent could involve the intermediacy of CH_3CN adducts, it was necessary to investigate whether electrode processes in this solvent were different to those reported previously.[1] In acetonitrile the first one-electron reduction process for $(CF_3)_2C_2Co_2(CO)_6$, corresponding to the formation of the radical anion, is seen at $E_{1/2} = -0.55$ V vs. Ag/AgCl ($E_p^r = -0.57$ V, $E^\circ_p = -0.49$ V) and is reversible ($E_{1/4} - E_{3/4} = 60$ mV, $i_p^a/i_p^c = 1$ at 500 mV s^{-1}) compared to −0.59 V in acetone. Additional electrode processes, not seen in acetone or CH_2Cl_2, were found at $E_{1/2} = -0.72$ V (ill-defined) and $E_{1/2} = -0.90$ V; in cyclic voltammograms the current due to the latter irreversible feature ($E_p^c = -0.82$ V) grew with repeated scanning and the associated redox couple is undoubtedly $[(CF_3)_2C_2Co_2(CO)_5(CH_3CN)]^{0/-\cdot}$ (vide infra). In contrast, there was only a small positive shift relative to acetone for the couple $Ph_2C_2Co_2(CO)_6{}^{0/-\cdot}$ in CH_3CN, and no features which could be attributed to a CH_3CN adduct. This is perhaps to be expected as the lifetime of the $Ph_2C_2Co_2(CO)_6^{-\cdot}$ radical anion is very short, but it is interesting that no substitution occurs on the electrochemical timescale at −70 °C, the temperature at which the radical anion can be detected by ESR.[9] Reaction via the alternative pathway involving mononuclear species[1] is apparently very fast and thermodynamically favored.

Other $RC_2R'Co_2(CO)_6$ compounds fall in between these two extremes of electrochemistry, the diffusion current due to a $[RC_2R'Co_2(CO)_5(CH_3CN)]^{0/-\cdot}$ couple increasing in importance as the electron-withdrawing capacity of R,R′ increases, that is, as the lifetime of $RC_2R'Co_2(CO)_6^{-\cdot}$ increases.

Preparation, Structure, and Reactivity of $(CF_3)_2C_2Co_2(CO)_5(CH_3CN)$. Electrochemical reduction of $(CF_3)_2C_2Co_2(CO)_6$ at −0.45 V vs. Ag/AgCl in acetonitrile under argon gave a red solution from which an air-stable deep red crystalline solid $(CF_3)_2C_2Co_2(CO)_5(CH_3CN)$ **1** was isolated in 70% yield. In an atmosphere of CO the yield drops to 20%. Alternatively, the electron for this ETC reaction can be provided by a chemical reducing agent, and with benzophenone ketyl (BPK) as the reductant, *a 100% yield of **1** is obtained within 1 min* in an argon atmosphere.

$$(CF_3)_2C_2Co_2(CO)_6 + CH_3CN \xrightarrow[\text{or BPK}]{-0.45\text{ V}} (CF_3)_2C_2Co_2(CO)_5(CH_3CN) + CO$$

The synthesis of **1** provides an excellent illustration of the ad-

Table V. Structural Parameters for Selected $(\mu\text{-}(R_2C_2))Co_2$ Complexes

compd	ref	Co-Co/Å	C≡C/Å	R-C-C/deg	
$(CF_3)_2C_2Co_2(CO)_5MeCN$	this work	2.465 (6)	1.35 (3)	136 (3)	136 (2)
$Ph_2C_2Co_2(CO)_6$	24a	2.460 (5)	1.36 (3)	141 (2)	141 (2)
$C_6F_6Co_2(CO)_6$	24b	2.488 (4)	1.36 (3)	119 (2)	123 (2)
$(CO)_9Co_3C(H)C_2Co_2(CO)_6$	24c	2.447 (4)	1.34 (2)	146 (1)	
$C_6Co_8(CO)_{24}$	24c	2.461 (8)	1.37 (3)	138 (2)	142 (2)
$(t\text{-Bu})_2C_2Co_2(CO)_6$	30a	2.463 (1)	1.335 (6)	144.5 (4)	144.8 (4)
$H_2C_2Co_2(CO)_4(PMe_3)_2$	30b	2.464 (1)	1.327 (6)	138	
$Ph_2C_2Co_2(CO)_4(triphos)$	25	2.512 (3)	1.36 (2)	138 (1)	140 (1)
$Ph_2C_2Co_2(CO)_4(dpm)$	26	2.459 (2)	1.33 (1)	137.7 (9)	143.2 (9)
$Ph_2C_2Co_2(CO)_2(dam)_2$	26	2.518	1.37 (3)	132 (2)	140 (2)

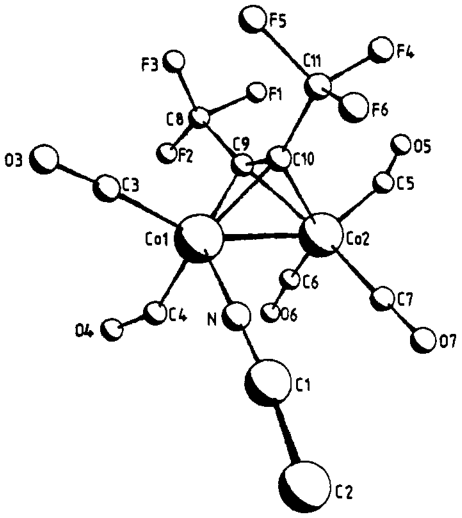

Figure 1. Perspective view of the molecule $(CF_3)_2C_2Co_2(CO)_5(CH_3CN)$.

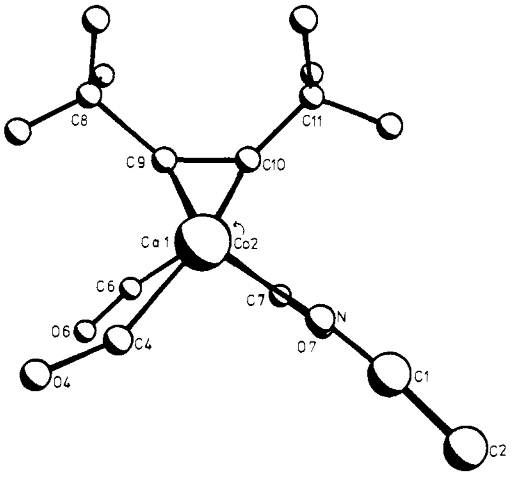

Figure 2. View of the molecule $(CF_3)_2C_2Co_2(CO)_5(CH_3CN)$ through the Co-Co bond.

vantages of ETC reactions since the *yield of 1 is only ~10% after 3 h in boiling acetonitrile.* Although the analytical and spectroscopic data supported the formulation as a CH_3CN adduct, an X-ray crystal structure analysis was undertaken in order to determine the coordination geometry of the CH_3CN group.

Structure. The crystal structure consists of discrete molecular units with the closest intermolecular contact between F1···O4 2.84 Å. A perspective view of the molecule is given in Figure 1 which also details the atom numbering scheme. In accord with observations for other molecules containing the dicobalt acetylene moiety,[24-26] the two cobalt atoms are linked by a metal-metal single bond. The observed Co1-Co2 bond length, 2.465 (6) Å, compares favorably with those found in the majority of other complexes with similar geometry (Table VI). It appears that the lengthening of the Co-Co bond, which has previously been observed[25,26] with the substitution of bulky ligands at cobalt, does not occur in this instance.

The coordination geometry around each cobalt atom can be described in terms of a distorted octahedron. Co1 carries the acetonitrile ligand on a pseudoequatorial site together with a pseudoaxial and pseudoequatorial carbonyl group, while Co2 has three carbonyl substituents. The alkyne carbon atoms of the acetylene are bound to each cobalt atom with the equatorial planes of the octahedra containing atoms N, C4, C9, C10 and C6, C7, C9, C10, respectively. The metal atoms Co1 and Co2 are displaced from these mean basal planes toward the pseudoaxial carbonyl groups by 0.38 and 0.25 Å, respectively. The acetonitrile ligand coordinates to Co1 in a linear fashion and the N-C1-C2 angle deviates only slightly from 180°. The Co-N distance is somewhat shorter than those observed in other acetonitrile complexes of Co(0)[27] and Co(I),[28] but the N-C1 and C1-C2 distances are unremarkable.

A surprising feature of acetonitrile coordination is the fact that the ligand replaces a pseudoequatorial and not a pseudoaxial carbonyl group. The crystal structure[30b] of the complex $H_2C_2Co_2(CO)_4(PMe_3)_2$ together with infrared[21,29] and NMR[27] evidence on a variety of "sawhorse" derivatives suggest that ligands of poorer π-acceptor ability than CO prefer the pseudoaxial sites. With this configuration the considerable nonbonded ligand interactions caused by the close Co-Co distance demanded by the acetylene interaction are minimized. In turn this relieves the repulsion between the filled a_1 orbital of the "sawhorse" $Co_2(CO)_6$ fragment and the filled a_1 acetylene donor orbital allowed by tilting of $(CO)_3Co\text{-}Co(CO)_3$ moiety.[11a] Substitution by a relatively small CH_3CN ligand in an equatorial configuration apparently engenders less repulsion than axial substitution. What effect the replacement of a π acceptor by a σ donor in the xz plane should have on the sawhorse-acetylene interaction is uncertain. Nonetheless, from a comparison of the structures of other "sawhorse" complexes it is clear that the steric requirements of the acetylene have a considerable influence on the orientation of the pseudoaxial substituents.[29,30] Figure 2, which views the molecule directly down the Co1-Co2 vector shows that the pseudoequatorial substituents remain in an approximately eclipsed conformation on substitution of one carbonyl group by MeCN. Some of the Co-C-O bonds depart significantly from linearity, but this is not unusual in metal carbonyl systems and may, in some measure, reflect the crystallographic disorder noted during the refinement of the structure.

---

(24) (a) Sly, W. G. *J. Am. Chem. Soc.* **1959**, *81*, 18-20. (b) Bailey, N. A.; Mason, R. *J. Chem. Soc. A* **1968**, 1293-1299. (c) Penfold, B. R.; Dellaca, R. J. *Inorg. Chem.* **1971**, *10*, 1269-1275.

(25) Bianchini, C.; Dapporto, P.; Meli, A. *J. Organomet. Chem.* **1979**, *174*, 205-212.

(26) Bird, P. H.; Fraser, A. R.; Hall, D. N. *Inorg. Chem.* **1977**, *16*, 1923-1931.

(27) Agnes, G.; Bassi, I. W.; Benedicenti, C.; Intrito, R.; Calcaterra, M.; Santini, C. *J. Organomet. Chem.* **1977**, *129*, 401-413.

(28) Albright, J. O.; Clardy, J. C.; Verkade, J. G. *Inorg. Chem.* **1977**, *16*, 1575.

(29) Varadi, G.; Vizi-Orozz, A.; Vastag, S.; Palyi, G. *J. Organomet. Chem.* **1976**, *108*, 225-233.

(30) (a) Cotton, F. A.; Jamerson, J. D.; Stults, B. R. *J. Am. Chem. Soc.* **1976**, *98*, 1774-1779. (b) Bonnet, J.-J.; Mathieu, R. *Inorg. Chem.* **1978**, *17*, 1973-1976.

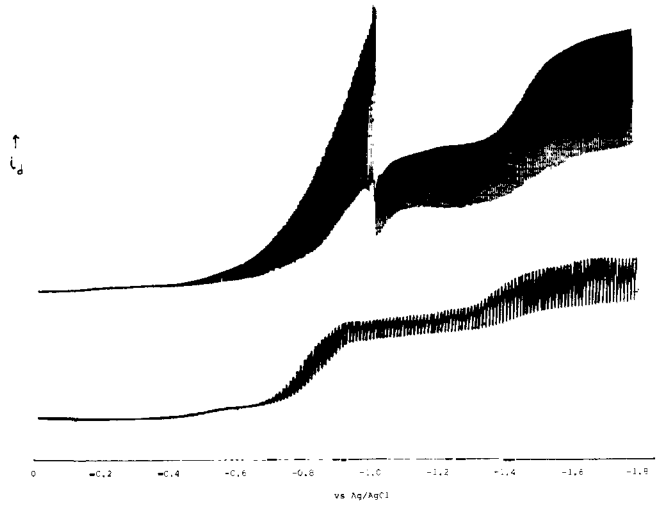

Figure 3. DC polarograms of 1.0×10^{-3} M $(CF_3)_2C_2Co_2(CO)_5(CH_3CN)$ measured in acetonitrile containing 0.1 M TEAP, scan rate 10 mV s^{-1} (a) at 298 K (b) 270 K. The same type of polarogram is obtained in CH_2Cl_2 and acetone.

Coordination of the $(CF_3)_2C_2$ ligand to the $Co_2(CO)_6$ system generates a tetrahedral unit with approximate C_2 symmetry. Figure 2 also illustrates the expected cis-bent conformation of the acetylene ligand. The C9–C10 bond is 1.35 Å long, in good agreement with the values reported for similar complexes (Table V), and the angles subtended by the CF_3 substituents [C8–C9–C10, 136 (3)°; C9–C10–C11, 136 (2)°] are relatively low corresponding to a "bend back angle" of 44°. It is tempting to suggest that this bending has its origin in electronic interactions, signifying stronger metal–acetylene bonding in the trifluoromethyl derivatives, but recent work[31] indicates that steric rather than electronic factors figure prominently in determining variations in bend back angle from a mean value of ~40°.

Spectroscopic and Electrochemical Data. Four of the five ν(CO) bands expected for this molecule of C_s symmetry are observed with the shift of 24 cm^{-1} in the A_1 mode[20] from that in $(CF_3)_2C_2Co_2(CO)_6$, reflecting the superior donor ability and weaker π-acceptor capability of MeCN relative to CO. No coordinated C≡N stretching mode was observed around 2280 cm^{-1}, but this is not unusual for MeCN complexes.[32] The coordinated CH_3CN is very labile, and solutions of **1** rapidly decompose if excess CH_3CN is not present. Nonetheless, high yields of $(CF_3)_2C_2Co_2(CO)_5L$ derivatives can be obtained via **1**. The rapid exchange between coordinated and solvent CH_3CN was manifested in the ^1H NMR spectrum by a shift of the sharp singlet at 2.30 ppm in $DCCl_3$, characteristic[33] of coordinated CH_3CN, to 1.96 ppm in CD_3CN. According to the crystal structure the two CF_3 groups are nonequivalent, but this was not evident in the ^{19}F NMR, although two singlets at 25.74 and 25.55 ppm (cf. 25.42 ppm for $(CF_3)_2C_2Co_2(CO)_6$) were observed with relative intensity 4:1. This suggests that **1** is stereochemically nonrigid in solution, existing as both equatorial and axial isomers, although the activation energy for the equatorial–axial interconversion must be considerably greater than that for CH_3CN exchange.[34]

DC polarograms and cyclic voltammograms ($E_{1/2} = -0.80$ V, $E_{1/4} - E_{3/4} = 70$ mV, $E_p^r = -1.05$ V on Pt, $E_p^r = -0.82$ V on Hg) are consistent with an irreversible one-electron reduction as the principal electrode process for **1**; this corroborates the assignments made for the electrode processes in $(CF_3)_2C_2Co_2(CO)_6/CH_3CN$ solutions (vide supra). Two aspects of the electrochemistry require comment. First, it is difficult to understand why radical anion formation from **1** is irreversible on Hg and Pt in all solvents when other $(CF_3)_2C_2Co_2(CO)_5L^{0/-}$ couples are at least quasi-reversible.[1] Second, at 298 K the polarograms feature large limiting currents per unit concentration (Figure 3) which do not vary with the height of the mercury column; these are features associated with a catalytic component.[35,36] The catalytic currents progressively decrease as the temperature is lowered while cyclic voltammograms on Pt are uncomplicated by abnormal currents or preabsorption waves. These observations suggest that the catalytic current is a consequence of the lability of the coordinated CH_3CN and of mercury intervention in the redox process. In this context, the polarograms at 298 K show another irreversible wave at $E_{1/2} = -1.29$ V (i_d equal to i_d for the couple **1**/**1**$^{-}\cdot$), which has no counterpart in the cyclic voltammograms on Pt; the i_d of this additional wave decreases in sympathy with the catalytic current at lower temperatures. Further work is in progress to identify the catalytic pathway in this system.

ETC Synthesis of $(CF_3)_2C_2Co_2(CO)_{6-n}L_n$. ETC syntheses, using a chemical reductant, gave the new derivatives $(CF_3)_2C_2Co_2(CO)_5L$ (L = $(MeO)_3P$, $(PhO)_3P$, Ph_3P, $(C_6H_{11})_3P$) in greater than 90% yields *within 1 min* at ambient temperature.

$$(CF_3)_2C_2Co_2(CO)_6 + L \xrightarrow[THF]{BPK} (CF_3)_2C_2Co_2(CO)_5L + CO$$

In comparison, yields from thermal reactions in boiling hexane over several hours varied from 10 to 60%, depending on the ligand and the propensity to form more highly substituted derivatives (Table I). ETC synthesis is therefore *highly selective, high in yield*, and *convenient*.

When the ETC reactions using BPK are carried out with $(CF_3)_2C_2Co_2(CO)_5L$ as substrates, further substitution will take place, but with lower yields. However, it was more convenient to produce $n = 2$, 3 derivatives in high yield by electrochemical reduction at a potential appropriate to the formation of the radical anion $(CF_3)_2C_2Co_2(CO)_5L^{-}\cdot$. Alternatively, electrochemical reduction at the trigger potential for $(CF_3)_2C_2Co_2(CO)_6^{-}\cdot$ gave the complete range of derivatives $(CF_3)_2C_2Co_2(CO)_{6-n}L_n$ (n = 1–3) within 5 min, the actual product yield depending on the $(CF_3)_2C_2Co_2(CO)_6$/nucleophile mole ratio (see Table II).

$$(CF_3)_2C_2Co_2(CO)_6 + nL \xrightarrow[MeCN]{-0.45\ V} (CF_3)_2C_2Co_2(CO)_{6-n}L_n$$

$$n = 1, 2\ (L = (MeO)_3P, (PhO)_3P, Ph_3P)$$

$$n = 3\ (L = (MeO)_3P, (PhO)_3P)$$

Possible structures for analogous derivatives $RC_2R'Co_2(CO)_{6-n}L_n$ (R = Ph, H, CH_2OH; R′ = Ph, Ph, CH_2OH, H) have been discussed in detail by Cullen and co-workers.[21] The infrared spectra show that monosubstitution gives the axial-substituted trifluoromethylacetylene derivatives, as is the case for the majority of $X_2M_2(CO)_5L$ complexes. In this structure nonbonded interactions between ligands are minimized (see discussion for $(CF_3)_2C_2Co_2(CO)_5(CH_3CN)$ above), which in turn allows the $Co_2(CO)_6$ sawhorse fragment to tilt in such a way as to relieve the repulsion between the filled $1a_1$ sawhorse orbital and the filled a_1 acetylene donor orbital. For $(CF_3)_2C_2Co_2(CO)_4L_2$ three ν(CO) bands are observed which is expected for the C_{2v} diaxial structure found[30b] for $H_2C_2Co_2(CO)_4(PMe_3)_2$; the ^1H and ^{19}F NMR spectra were also consistent with this geometry. $(CF_3)_2C_2Co_2(CO)_3[(MeO)_3P]_3$ is characterized by one sharp and one broad ν(CO) band although three bands are expected for the C_s (diequatorial, axial) or C_1 (diaxial, equatorial) isomers. The ^1H NMR spectrum shows that there are two sets of $(MeO)_3P$ ligands (ratio 1:2) while the ^{19}F NMR spectrum, after ^1H decoupling, shows that the CF_3 groups on the acetylene moiety are nonequivalent (a quartet and a complex multiplet are observed). These data suggest that the

---

(31) Farrar, D. H.; Payne, N. C. *Inorg. Chem.* **1981**, *20*, 821–828.

(32) Hensley, D. W.; Stewart, R. P. *Inorg. Chem.* **1976**, *15*, 2418–2421.

(33) Regina, F. J.; Wojcicki, A. *Inorg. Chem.* **1980**, *12*, 3803.

(34) Low-temperature ^1H and ^{19}F NMR data are inconclusive on this point.

(35) Bond, A. "Modern Polarographic Methods in Analytical Chemistry"; Marcel Dekker: New York, 1980.

(36) The possibility that the large limiting currents were due to resistance phenomena arising from physical oscillation or desorption on the electrode surface was considered but rejected because they were unaffected by a large resistance (100–1000 Ω) placed in series with the working electrode. Similar catalytic-type diffusion currents were noted in the polarograms of some $(CF_3)_2C_2Co_2(CO)_5L$ derivatives.

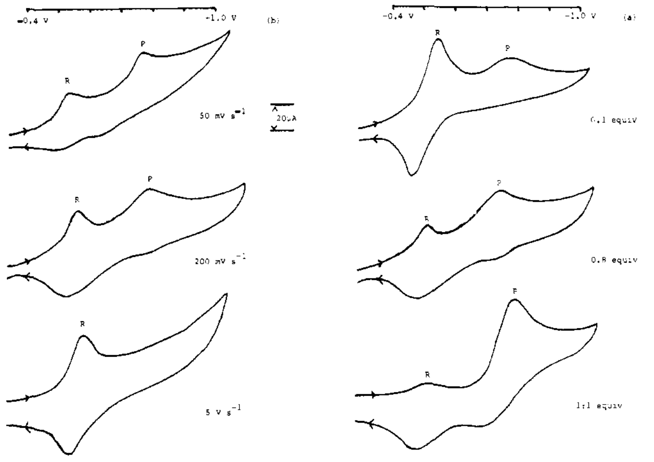

Figure 4. Cyclic voltammograms of 0.88 × 10^{-3} M $(CF_3)_2C_2Co_2(CO)_6$ measured in acetone containing 0.1 M TEAP at 293 K: (a) in the presence of the varying amounts of Ph_3P indicated on the figure at 200 mV s^{-1}: R & P refer to the peak potentials of $(CF_3)_2C_2Co_2(CO)_6$ and $(CF_3)_2C_2Co_2(CO)_5(Ph_3P)$, respectively; (b) sweep rate dependence at a 0.5 equiv ligand concentration.

trisubstituted product has the diaxial, equatorial configuration.

Chain Mechanism for Ligand Substitution. High yields, rapid reaction, low consumption of electricity (<0.1 faraday/mol of substrate), and high current or reductant efficiencies characterize these nucleophilic substitution reactions of $(CF_3)_2C_2Co_2(CO)_6$ as genuine examples of bulk ETC processes which take place in the absence of thermal exchange. The main factor controlling the efficiency of the chain process is the rate of nucleophilic attack compared to that for the chain-terminating (especially transient) steps. An insight into these different rates is provided by the transient electrochemical behavior for multiple-ligand electrocatalytic substitution, such as the cyclic voltammograms shown in Figures 4 and 5 for the reaction of $(CF_3)_2C_2Co_2(CO)_6$ with Ph_3P. On the addition of 0.3 equiv of ligand, the cathodic current due to $(CF_3)_2C_2Co_2(CO)_6$ is decreased by 22% at a scan rate of 200 mV s^{-1}, accompanied by a slight positive shift of 0.07 V in the cathodic peak potential (from $E_p^c = -0.62$ V), together with the appearance of a new wave at −0.78 V ascribed to the formation of $(CF_3)_2C_2Co_2(CO)_5(Ph_3P)$[1] (Figure 4a). At 5 V s^{-1} only the parent reversible reduction couple is observed; at 50 mV s^{-1} the two couples are observed but the reactant couple is irreversible ($i_a^P/i_c^P \ll 1$), (Figure 4b). This data is consistent with a catalytic ECE mechanism. Incremental addition of further ligand leads to further diminution of the reactant wave and finally complete disappearance of the reactant wave at 1.4 equiv of ligand (there is a small current due to the $(CF_3)_2C_2Co_2(CO)_4(Ph_3P)_2{}^{0/-}$ couple at this stage not shown in Figure 4); at the same time the cathodic potential of the product wave remains constant and becomes quasi-reversible (Figure 4b). These results imply that the nucleophilically substituted anion is able to escape from the electrode layer and trigger, very efficiently, the chain process in the diffusion layer and in the bulk of the solution. Consequently, the rate of nucleophilic attack must be exceptionally fast, although it must be dependent on the type of ligand as the disappearance of the reactant wave requires different ligand to nucleophile ratios [$P(OMe)_3$, 1.1 equiv; $P(C_6H_{11})_3$, 2.1 equiv].

Another appreciation of this rate can be obtained from the repetitive scans shown in Figure 5. The number of scans required to deplete the diffusion layer of a reactant, for a specific ligand concentration, is a function of the scan rate and the nucleophilicity of the ligand. Under constant electrochemical conditions[37] the number of scans required for depletion of reactant can be taken as a measure of the rate of nucleophilic attack. The order established from this transient electrochemical data is $P(OR)_3 > PPh_3 > P(C_6H_{11})_3$, exactly the same efficiency order established for the bulk catalytic process (vide infra). The same conclusion can be drawn from measurements of the ligand dependence of polarographic diffusion currents. Thus, a plot of log i_d^r vs. [Nu] or log i_d^p vs. [Nu] (r, reactant; p, product) is linear, and while the reason for this relationship is open to conjecture, the slopes of these plots were reproducible for a given nucleophile, solvent, and temperature and were independent of drop time. Without placing too much emphasis on these data, one may regard the slopes and [Nu] at maximum i_d^p as a measure of the efficiency of $[(CF_3)_2C_2Co_2(CO)_5Nu]^{-\cdot}$ in propagating the chain process; as expected, this gives the same "efficiency order" noted in cyclic voltammograms.

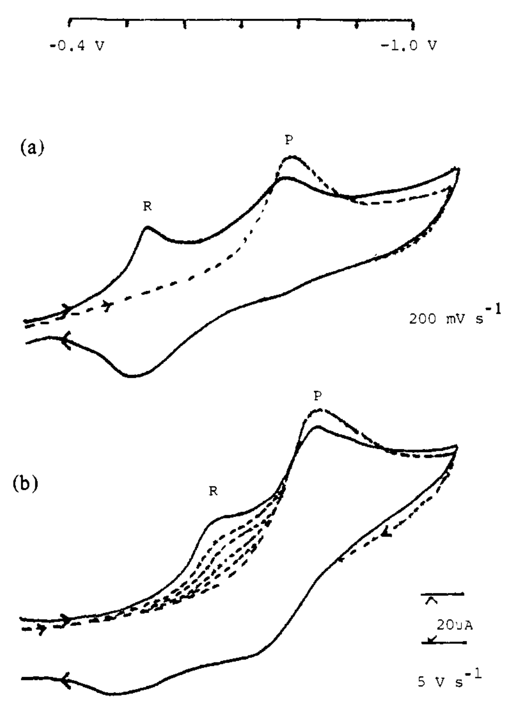

Figure 5. Repetitive cyclic voltammograms of 0.88 × 10^{-3} M $(CF_3)_2C_2Co_2(CO)_6$; measured in acetone containing 0.1 M TEAP at 293 K in the presence of 0.5 equiv of Ph_3P at sweep rate (a) 200 mV s^{-1}, (b) 5 V s^{-1}.

On a preparative scale, yields can be taken as a measure of the relative rate of nucleophilic attack if the chain is long, i.e., if the chain-terminating fragmentation pathways do not effectively compete with the electron-transfer chain. That this is so is demonstrated by the high current efficiencies. The data in Table II suggest that the nucleophilic efficiency in the chain is related to the capacity of the nucleophile to relieve the charge density on the cobalt atoms in $(CF_3)_2C_2Co_2(CO)_5Nu^{-\cdot}$ (i.e., its "softness") and the bulk of the nucleophile, in accord with the electrochemical interpretation. It is interesting that this same trend has been noted in $S_{RN}1$ reactions with aromatic substrates and a more comprehensive study with a wider variety of nucleophiles is underway to establish its generality with polynuclear metal carbonyl substrates.

The number of nucleofugal groups displaced in the ETC reactions is also influenced by the nucleophile and is restricted compared to thermal synthesis. For instance, $(CF_3)_2C_2Co_2(CO)_2[(MeO)_3P]_4$ is readily synthesised in boiling hexane, but the limit of substitution by ETC is $(CF_3)_2C_2Co_2(CO)_3[(MeO)_3P]_3$; with Ph_3P the chain stops at $(CF_3)_2C_2Co_2(CO)_4(Ph_3P)_2$. Chain termination of the stepwise ETC nucleophilic substitution coincides with a relatively short lifetime for the appropriate radical anion in the chain (i.e., $[(CF_3)_2C_2Co_2(CO)_3[(MeO)_3P]_3]^{-\cdot}$; $[(CF_3)_2C_2Co_2(CO)_4(Ph_3P)_2]^{-\cdot}$). A point must be reached where the extra charge density on the cobalt atoms provides the impetus

---

[37] By use of an electrode, the overall rate is a function of the heterogeneous rate constants for the two redox couples involved and the homogeneous rate constant for nucleophilic attack. It should be appreciated that, at the potentials used for the electrocatalyzed reactions, oxidation of the nucleophilically substituted radical anion by the electrode will take place. However, the outer-sphere electron transfer is faster than the heterogeneous rate constant.

Table VI. Examples of Electron-Induced Nucleophilic Substitution of Polynuclear Carbonyls[a]

substrate	nucleophile (L)	product	yield[b]
$Fe_2(CO)_9$	$P(OPh)_3$	$Fe(CO)_4L$	50[c]
	PPh_3	$Fe(CO)_4L$	30[c]
$Fe_3(CO)_{12}$	$P(OMe)_3$	$Fe(CO)_4L$	60
	$P(OPh)_3$	$Fe(CO)_4L$	55
	$P(OMe)_3$	$Fe_3(CO)_{11}L$	75[d]
	PPh_3	$Fe_3(CO)_{11}L$	60[d]
$Ru_3(CO)_{12}$	MeCN	$Ru_3(CO)_{11}L$	65
	$P(OMe)_3$	$Ru_3(CO)_{11}L$	80
	dpm	$Ru_3(CO)_{10}L$	75
$Os_3(CO)_{12}$	MeCN	$Os_3(CO)_{11}L$	70
	$P(OMe)_3$	$Os_3(CO)_{11}L$	90
$(CF_3)_2C_2Co_2(CO)_6$	$P(OMe)_3$	$(CF_3)_2C_2Co_2(CO)_5L$	100
	dpm	$(CF_3)_2C_2Co_2(CO)_4L$	100
	ttas	$(CF_3)_2C_2Co_2(CO)_4L$	100
$[(CF_3)_2C_2]_3Co_2(CO)_4$	MeCN	$[(CF_3)_2C_2]_3Co_2(CO)_3L$	100
	dpm	$[(CF_3)_2C_2]_3Co_2(CO)_2L$	90
	$P(OMe)_3$	$[(CF_3)_2C_2]_3Co_2(CO)_2L_2$	100*[e]
$PhCCo_3(CO)_9$	MeCN	$PhCCo_3(CO)_8L$	90*
	dpm	$PhCCo_3(CO)_7L$, $PhCCo_3(CO)_8L$	*f*
	PPh_3	$PhCCo_3(CO)_8L$	90
	$CpMo(CO)_3^-$	$PhCCo_2Mo(CO)_8(Cp)$	90
$Ir_4(CO)_{12}$	PPh_3	$Ir_4(CO)_{11}L$	90

[a] Solvent: THF or MeCN; 293 K, unless otherwise specified. [b] Yields are averaged from several preparations and rounded to the nearest ±5%; yields are from BPK initiation except those marked with an asterisk which are electrocatalyzed. The procedure was as described in this paper for reactions of $R_2C_2Co_2(CO)_6$. [c] Small amounts of $Fe(CO)_3L_2$ are also formed; note that the addition of BPK effectively solubilizes $Fe_2(CO)_9$. [d] At low temperatures, ~253 K. [e] The purple isomer. [f] Yields of each compound vary from 50 to 90% depending on conditions.

for an increased rate of disproportionation and fragmentation relative to nucleophilic substitution. It is possible that the stereospecific nucleophilic attack is slower with Ph_3P and $(C_6H_{11})_3P$ because of the bulk of the nucleophile.

From a mechanistic point of view it is important to consider why nucleophilic attack on the radical anion is exceedingly fast compared to that on the neutral species, how the nucleophile influences the rate of reaction, and why CO in solution has a deleterious effect on the yield. This last observation in an Fe_3 system led to a suggestion[6] that the rate-determining step in ETC reactions with metal carbonyl substrates is CO dissociation from the radical anion, followed by rapid nucleophilic attack and electron transfer.

Initiation:

$$(CF_3)_2C_2Co_2(CO)_6 + e \rightleftharpoons (CF_3)_2C_2Co_2(CO)_6^{-}\cdot$$

$$(CF_3)_2C_2Co_2(CO)_6^{-}\cdot \xrightarrow{\text{slow}} (CF_3)_2C_2Co_2(CO)_5^{-}\cdot + CO$$

$$(CF_3)_2C_2Co_2(CO)_5^{-}\cdot + Nu \overset{\text{fast}}{\rightleftharpoons} (CF_3)_2C_2Co_2(CO)_5Nu^{-}\cdot$$

Propagation:

$$(CF_3)_2C_2Co_2(CO)_5Nu^{-}\cdot + (CF_3)_2C_2Co_2(CO)_6 \rightarrow (CF_3)_2C_2Co_2(CO)_5Nu + (CF_3)_2C_2Co_2(CO)_6^{-}\cdot$$

Alternatively, the initiation step could include an activation barrier which involves the stretching or cleavage of the Co–Co bond followed by nucleophilic attack at a coordinatively unsaturated metal center (the propagation step would be the same as above).

Initiation:

$$(CF_3)_2C_2Co_2(CO)_6 + e \rightarrow (CF_3)_2C_2Co_2(CO)_6^{-}\cdot$$

$$(CF_3)_2C_2Co_2(CO)_6^{-}\cdot \overset{\text{slow}}{\rightleftharpoons} (CF_3)_2C_2(CO)_3Co(\mu\text{-}CO)Co^{-}\cdot(CO)_2$$

$$(CF_3)_2C_2(CO)_3Co(\mu\text{-}CO)^{-}\cdot Co(CO)_2 + Nu \rightarrow [(CF_3)_2C_2Co_2(CO)_5Nu^{-}\cdot + CO]$$

The product yield, or the cyclic voltammetric behavior, from this type of initiation will also be dependent on the [CO], providing the rate of electron transfer in the propagating step and nucleophilic attack at the coordinatively unsaturated metal center is fast. There will thus be competition between CO and the alternative nucleophile for the vacant coordination site with CO coordination effectively acting as a chain-terminating step. Both mechanistic paths would therefore predict dependence of the product yield on [CO], yet there is compelling circumstantial evidence for Co–Co bond cleavage in the transition state. The inherent lability of metal–metal bonds has been widely recognized[38,39] and facile M–M cleavage forms the basis for a number of synthetic strategies in metal cluster chemistry.[40] Metal–CO bond enthalpies are generally greater than metal–metal bond enthalpies;[41] radical anion formation, where the unpaired electron enters an antibonding, metal-centered orbital should further encourage M–M cleavage. A corollary to this observation is the fact that a marked reduction in $\nu(CO)$ in a variety of cluster radical anion systems[16] indicates that radical anion formation tends to strengthen the M–CO bond at the expense of the M–M interaction. Furthermore, a marked diminution in the rate of nucleophilic substitution with increased negative charge on the cluster moiety has been observed in diamagnetic cluster systems such as $FeCo_3(CO)_{12}^-/FeCo_3(CO)_{12}H$;[42] such observations have been ascribed to an increase in back-donation with associated increase in M–CO bond energy in the anion. Finally, lifetimes of the radical anions $R_2C_2Co_2(CO)_6^{-}\cdot$ are found to be independent of CO or alternative nucleophile concentration[1] which lends strong support to the second mechanism.

ETC Reactions with Other $RC_2R'Co_2(CO)_6$ Substrates. The lifetime of the $RC_2R'Co_2(CO)_6^{-}\cdot$ radical anions is a function of the electronegativity of R, R′. At room temperature the lifetime for R, R′ = CF_3 is estimated to be >1 h while that for $t\text{-}Bu_2C_2Co_2(CO)_6^{-}\cdot$ is 70 ms. The nadir of kinetic stability is reached when R, R′ = Ph when the lifetime is 17 ms. From these data ETC reactions with $Ph_2C_2Co_2(CO)_6$ should not have extended

---

(38) (a) Madach, T.; Vahrenkamp, H. *Z. Naturforsch.* **1979**, *34б*, 573–578. (b) Beurich, H.; Madach, T.; Richter, F.; Vahrenkamp, H. *Angew. Chem., Int. Ed. Engl.* **1979**, *18*, 690–691.

(39) (a) Jackson, R. A.; Poe, A. *Inorg. Chem.* **1979**, *18*, 3331–3333. (b) Bernard, M. *J. Am. Chem. Soc.* **1978**, *100*, 7740–7742. (c) Roberts, D. A.; Mercer, W. C.; Zahurak, S. M.; Geoffroy, G. L.; DeBrosse, C. W.; Cass, M. E.; Plepont, C. G. *Ibid.* **1982**, *104*, 910–913.

(40) (a) Eckehart, R.; Vahrenkamp, H. *Angew. Chem., Int. Ed. Engl.* **1981**, *20*, 679–680. (b) Vahrenkamp, H.; Wucherer, E. J. *Ibid.* **1981**, *20*, 680–681. (c) Marinetti, A.; Sappa, E.; Tripiechio, A.; Camelline, M. T. *Inorg. Chim. Acta* **1980**, *44*, L183–L184.

(41) Connor, C. A. "Transition Metal Clusters"; Johnson, B. F. G., Ed.; Wiley: England, 1980; 183–184.

(42) Cook, C. G.; Mays, M. J. *J. Organomet. Chem.* **1974**, *74*, 449–455.

chain lengths, and indeed the electrochemical data suggest that the substitution pathway accounts for ~50% and ~70% of the overall reaction with PPh_3 and $P(OMe)_3$, respectively.[1] Since the chain length is only 2 or 3, a considerable amount of reducing agent would be required for the complete conversion of substrate.

Nevertheless, at 293 K the results from bulk electron-induced reactions with BPK were discouraging and only phosphites gave significant products (~10% yield). This illustrates the danger in extrapolating from electrochemical data, where the reaction is taking place close to the electrode surface, to homogeneous solution reactions. The heterogeneous electrode could well play a significant role in some chain processes (witness the different electrochemistry with Pt and Hg electrodes), and in fact, electrocatalysis in bulk at carefully controlled potentials did increase the yields of $Ph_2C_2Co_2(CO)_{5-n}L_n$ derivatives. Although better yields were achieved by carrying out the BPK initiated reactions at lower temperatures, ETC reactions offer no advantages over thermal methods with this substrate.

As the lifetime of the $RC_2R'Co_2(CO)_6^{-}\cdot$ increases the ETC route becomes more viable and this is indicated by the results in Table II.

Electron-Induced Reactions of Polynuclear Carbonyls. Electron-induced reactions of polynuclear metal carbonyls in many cases offer a more selective higher yield synthesis than achieved by thermal, photochemical, or oxidative (Me_3NO) methods (Table VI).[43] In subsequent papers some of these will be analyzed in detail, but here we wish to clarify and extend the results independently reported by Bruce and co-workers.[5b,44]

It should be emphasized that efficient ETC processes are not involved in many reactions given in Table VI. For example, $Ru_3(CO)_{12}$ and $Os_3(CO)_{12}$ are unlikely to participate in uncomplicated ETC reactions based on $M_3(CO)_{12}^{-}\cdot$ as the lifetime of these radical anions is very short.[14b] With these particular substrates fragments of higher and lower nuclearity participate in the redox process and may indeed be the catalysts, hence the apparent "catalytic" amount of BPK required (cf. reactions of $Fe(CO)_5$).[45] Both $Ru_3(CO)_{12}$ and $Os_3(CO)_{12}$ themselves react with BPK,[46] but the chain length for pathways involving $M_3(CO)_{12}^{-}\cdot$ can be increased by lowering the reaction temperature (see reaction of $Fe_3(CO)_{12}$).

Sequential substitution of CO in a cluster[6] does take place with BPK, but the extent of this sequence is determined by the nucleophile and the lifetime of the intermediate radical anions. As a general rule, only the first substitution is an efficient ETC reaction. Furthermore, sequential substitution by either a monodentate or polydentate ligand is stereospecific if a chain process is involved, a fact that can be utilized to produce an isomeric distribution not achievable by other methods.[48] As an example, the reaction of dppe with $YCCo_3(CO)_9$ proceeds via a very efficient stereospecific ETC process to the "dangling" product where one end of the ligand only is coordinated, whereas the "zipping up" to give a bidentate derivative is a stoichiometric nonstereospecific electron-induced step (1 F/mol^{-1}).[43]

Finally, by use of metal-centered nucleophiles EINS and ETC reactions can be used to systematically generate metal clusters;[49] one example, the preparation of a heteronuclear cluster, is given in Table VI.

Table VII. Final Positional and Thermal Parameters for $(CF_3)_2C_2Co_2(CO)_5(MeCN)$

atom	x/a	y/b	z/c	U_{11}
Co1	0.8143	0.9680	1.1968	0.0436
	0.0004	0.0007	0.0000	0.0032
Co2	0.8107	0.9698	0.9715	0.0786
	0.0006	0.0008	0.0005	0.0055
N	0.6950	0.9914	1.2140	0.1064
	0.0032	0.0055	0.0061	0.0170
C1	0.6197	0.9919	1.2231	0.0937
	0.0040	0.0060	0.0062	0.0193
C2	0.5261	1.0164	1.2580	0.1310
	0.0034	0.0051	0.0062	0.0179
C3	0.8349	0.8955	1.3441	0.1795
	0.0052	0.0093	0.0055	0.0385
C4	0.8553	1.1345	1.2228	0.2497
	0.0061	0.0061	0.0100	0.0515
C5	0.8396	0.8869	0.8351	0.0383
	0.0020	0.0037	0.0029	0.0101
C6	0.8504	1.1362	0.9469	0.0479
	0.0023	0.0028	0.0036	0.0114
C7	0.6960	0.9861	0.9435	0.0414
	0.0027	0.0043	0.0040	0.0109
C8	0.9890	0.8591	1.0978	0.0936
	0.0023	0.0041	0.0075	0.0122
C9	0.8933	0.8887	1.0748	0.0454
	0.0016	0.0025	0.0049	0.0076
C10	0.8203	0.8187	1.0856	0.0452
	0.0015	0.0024	0.0053	0.0066
C11	0.7960	0.6746	1.0927	0.0756
	0.0021	0.0033	0.0079	0.0094
O3	0.8393	0.8329	1.4310	0.1092
	0.0023	0.0036	0.0029	0.0126
O4	0.8880	1.2270	1.2656	0.1946
	0.0036	0.0044	0.0052	0.0247
O5	0.8760	0.8351	0.7594	0.1167
	0.0021	0.0035	0.0031	0.0131
O6	0.8735	1.2464	0.9427	0.0861
	0.0020	0.0027	0.0031	0.0105
O7	0.6323	1.0017	0.9348	0.0861
	0.0028	0.0040	0.0035	0.0127
F1	1.0115	0.8157	0.9775	0.0917
	0.0015	0.0025	0.0025	0.0079
F2	1.0269	0.9707	1.1181	0.1232
	0.0014	0.0025	0.0030	0.0093
F3	1.0046	0.7634	1.1602	0.1263
	0.0020	0.0031	0.0031	0.0118
F4	0.8049	0.6122	0.9787	0.0913
	0.0015	0.0025	0.0024	0.0080
F5	0.8430	0.6028	1.1711	0.0812
	0.0014	0.0023	0.0023	0.0074
F6	0.7144	0.6560	1.1088	0.1133
	0.0013	0.0022	0.0033	0.0084

atom	U_{22}	U_{33}	U_{23}	U_{13}	U_{12}
Co1	0.0626	0.0431	0.0101	0.0141	−0.0163
	0.0053	0.0037	0.0036	0.0038	0.0040
Co2	0.0588	0.0739	0.0278	0.0180	0.0101
	0.0053	0.0065	0.0039	0.0044	0.0050

Conclusion

The scope of electron-induced nucleophilic substitution appears to be general for polynuclear metal carbonyl substrates, and it should become an important synthetic tool in organometallic chemistry. Whether at ETC mechanism will prevail depends on the lifetime of the radical anion and, to a lesser extent, on the nucleophile. However, it is clear that a number of mechanistic questions need to be answered before the full potential of this technique is realized and further work in this area is under way.

---

(43) Solvents and the concentration of BPK were as described in this paper and all known compounds were characterized by spectroscopic data; new compounds had satisfactory analytical and spectroscopic data. The yields refer to BPK reactions, but it should be noted that higher yields of sequentially substituted products can be obtained from electrocatalysis at the appropriate trigger potential. The work was carried out at the University of Otago by A. Downard and S. Jensen.

(44) We are grateful to Professor Bruce and Dr. Nicholson for preprints of their work.

(45) Butts, S. B.; Shriver, D. F. *J. Organomet. Chem.* **1979**, *169*, 191–197.

(46) Electrochemical reduction of these clusters also generates a range of clusters as well as the paramagnetic mononuclear species detected by ESR methods.[14b] It is not surprising that the products obtained, e.g., $Ru_6(CO)_{18}^{2-}$, are related to those obtained from the reduction reactions investigated by Shore and co-workers.[47]

(47) Nagel, C. C.; Shore, S. G. *J. Chem. Soc., Chem. Commun.* **1980**, 530–531.

(48) Arewgoda, M.; Robinson, B. H.; Simpson, J. *J. Chem. Soc., Chem. Commun.* **1982**, 284–285.

(49) Jensen, S.; Robinson, B. H.; Simpson, J. *J. Chem. Soc., Chem. Commun.*, submitted for publication.

Acknowledgment is made to the donors of the Petroleum Research Fund, administered by the American Chemical Society, for partial support of this work. We thank Professors A. M. Bond and P. H. Rieger for their interest and advice.

Supplementary Material Available: Listing of observed and calculated structure factors for $(CF_3)_2C_2Co_2(CO)_5(MeCN)$ (8 pages). Ordering information is given on any current masthead page.

Electrochemical Reduction of the Gold Cluster $Au_9(PPh_3)_8^{3+}$. Evidence for an $E_rE_rC_r$ Mechanism. Formation of the Paramagnetic Gold Cluster $Au_9(PPh_3)_8^{2+}$

J. G. M. van der Linden,* M. L. H. Paulissen, and J. E. J. Schmitz

Contribution from the Department of Inorganic Chemistry, University of Nijmegen, Toernooiveld, 6525 ED Nijmegen, The Netherlands. *Received July 12, 1982*

Abstract: The gold cluster compound $Au_9(PPh_3)_8^{3+}$ can be reduced at a platinum electrode in various solvents (CH_3CN, CH_2Cl_2, acetone). Controlled potential electrolysis delivered $n = 2$. In acetonitrile the unipositive gold cluster compound $Au_9(PPh_3)_8PF_6$ precipitated on the electrode, thus providing a method for larger scale preparation. Application of recently developed theories of pulse and cyclic voltammetry and convolution of linear sweep and cyclic voltammetry shows that the reduction in acetone follows an EE reaction path with $E_{1/2}(1) = -0.36$ V and $E_{1/2}(2) = -0.40$ V vs. a Ag-AgCl reference electrode. From the difference in half-wave potentials, it follows that the conproportionation constant $K_c = 4.7$ for the equilibrium $Au_9(PPh_3)_8^{3+} + Au_9(PPh_3)_8^{+} \rightleftharpoons 2Au_9(PPh_3)_8^{2+}$ and that in mixing the 3+ and 1+ ions in a 1:1 molar ratio a large amount of the paramagnetic 2+ cluster should be formed. Indeed, an ESR experiment conducted at 20 K revealed a signal at $g_{av} = 1.982$.

In recent years interest in this[1] and other laboratories[2] has focused on the preparation, characterization, molecular structure determination, and reactivity of gold cluster compounds. In contrast with most other metal clusters containing carbonyl as the prominent ligand,[3] the peripheral atoms in these gold clusters are coordinated with tertiary phosphines.

These gold clusters show a large variety of interconversion reactions. The $Au_9(PPh_3)_8^{3+}$ cluster is a key compound in this sense, and e.g., reactions have been described with PPh_3, I^-, $Ph_2PCH_2PPh_2$, Cl^-, and SCN^- which lead to clusters with 8, 4, 5, and 11 gold atoms, respectively.[1]

No detailed electrochemical studies on these gold cluster compounds have been reported, although preliminary results have appeared.[4,5]

In this paper we present a detailed electrochemical study of the two-electron reduction of the $Au_9(PPh_3)_8^{3+}$ cluster which follows a EE reaction path. In addition, evidence will be given for the existence of the paramagnetic gold cluster $Au_9(PPh_3)_8^{2+}$.

Experimental Section

Measurements. Electrochemical measurements were made with a three-electrode Bruker E310 instrument or a PAR Polarographic Analyzer Model 174A coupled with a Universal Programmer PAR Model 175. The working electrode was a platinum disk, the auxiliary electrode a platinum plate, and the reference electrode a Ag-AgCl (0.1 M LiCl-acetone) electrode separated from the test solution via a Luggin capillary containing the supporting electrolyte (0.1 M Bu_4NPF_6). The Luggin capillary was positioned as close as possible (within 0.5 mm) to the working electrode to minimize *iR* drop. No external *iR* compensation was employed. Normal and differential pulse voltammograms were obtained at a scan rate of 5 mV/s with a pulse frequency of 2.0 pulses s^{-1}; the differential amplitude was 10 mV. Cyclic voltammograms were taken with scan rates of 0.05–50 V/s. The recording device was a Kipp BD 30 recorder, while cyclic voltammograms with scan speeds larger than 200 mV/s were displayed on a Tektronix 564B storage oscilloscope or a Nicolet Explorer II Model 206. Controlled potential electrolyses were carried out with a Wenking LB 75M potentiostat and a Birtley electronic integrator. Complete electrolysis of about 25 mg of electroactive material generally required 50 min. The temperature of the electrochemical measurements was 25 ± 1 °C.

AC voltammetry was carried out on a platinum disk, using a PAR 175A instrument coupled via a PAR 174/50 interface with a PAR Model 5204 lock-in amplifier with a built-in oscillator. Frequencies were measured with a HP 5381 frequency counter. The interface was modified in such a way that the amplitude of the applied voltage can be adjusted to every value between 0–30 mV. Measurements were made with an amplitude of 4 mV peak to peak in the frequency range 25–700 Hz, due to the frequency limit of the PAR 174A instrument.

$^{31}P\{^1H\}$ NMR spectra were recorded on a Varian XL-100 FT instrument at a frequency of 40.5 MHz with TMP as the internal reference. Electron spin resonance experiments were carried out on a Varian E12 instrument. All measurements were carried out under a nitrogen atmosphere.

Materials. All the reagents used were of reagent quality. $Au_9(PPh_3)_8(PF_6)_3$ was prepared as described either by the reduction of $Au(PPh_3)NO_3$ with $NaBH_4$ in ethanol[6] or by evaporation of metallic gold into an ethanolic solution of PPh_3 and NH_4PF_6.[7] $Au_9(PPh_3)_8PF_6$ was obtained from controlled potential electrolyses (−0.60 V) in acetonitrile solutions of about 50 mg of the $Au_9(PPh_3)_8^{3+}$ cluster compound. The $Au_9(PPh_3)_8^{+}$ cluster was isolated by repeatedly scraping off the product from the electrode and recrystallizing from CH_2Cl_2–diethyl ether mixtures.

Diffusion Coefficient. The diffusion coefficient of the $Au_9(PPh_3)_8^{3+}$ cluster ($c = 5.2 \times 10^{-4}$ M) was obtained from the analysis of the chronoamperometric i–t transient[8] according to eq 1. These measurements

$$it^{1/2} = nFAC(D/\pi)^{1/2} \qquad (1)$$

shows a constant value for $it^{1/2} = 40.4$ A $s^{1/2}$ in the time range 1.8–4.5

---

(1) For a recent review, see: Steggerda, J. J.; Bour, J. J.; Van der Velden, J. W. A. *Recl. Trav. Chim. Pays-Bas* **1982**, *101*, 164.

(2) Demartin, F.; Mannasero, M.; Naldini, J.; Ruggeri, R.; Sansoni, M. J. *J. Chem. Soc., Chem. Commun.* **1981**, 222.

(3) Chini, P. *J. Organomet. Chem.* **1980**, *200*, 37.

(4) Vollenbroek, F. A. Ph.D. Thesis, University of Nijmegen, 1979.

(5) van der Linden, J. G. M.; Paulissen, M. L. H.; Schmitz, J. E. J. *Ext. Abstr., Meet. Int. Soc. Electrochem. 33rd* **1982**, 630.

(6) Cariati, F.; Naldini, L. *J. Chem. Soc., Dalton Trans.* **1972**, 2286.

(7) Vollenbroek, F. A.; Bour, J. J.; Van der Velden, J. W. A. *Recl. Trav. Chim. Pays-Bas* **1980**, *99*, 137.

(8) Adams, R. N. "Electrochemistry at Solid Electrodes"; Marcel Dekker: New York, 1969; Chapter 8.

0002-7863/83/1505-1903$01.50/0